

Comparison of various density functional methods for distinguishing stereoisomers based on computed ^1H or ^{13}C NMR chemical shifts using diastereomeric penam β -lactams as a test set

Keith W. Wiitala, Christopher J. Cramer and Thomas R. Hoye*

Department of Chemistry and Supercomputer Institute, University of Minnesota, 207 Pleasant St. SE, Minneapolis, MN 55455-0431, USA

Received 7 May 2007; Accepted 30 May 2007



Full ^1H and ^{13}C NMR chemical shift assignments were made for two sets of penam β -lactams: namely, the diastereomeric (2*S*, 5*S*, 6*S*)-, (2*S*, 5*R*, 6*R*)-, (2*S*, 5*S*, 6*R*)-, and (2*S*, 5*R*, 6*S*)-methyl 6-(1,3-dioxoisindolin-2-yl)-3,3-dimethyl-7-oxo-4-thia-1-aza-bicyclo[3.2.0]heptane-2-carboxylates (1–4) and (2*S*, 5*R*, 6*R*)-, (2*S*, 5*S*, 6*R*)-, and (2*S*, 5*R*, 6*S*)-6-(1,3-dioxoisindolin-2-yl)-3,3-dimethyl-7-oxo-4-thia-1-aza-bicyclo[3.2.0]heptane-2-carboxylic acids (6–8). Each penam was then modeled as a family of conformers obtained from Monte Carlo searches using the AMBER* force field followed by IEFPCM/B3LYP/6-31G(d) geometry optimization of each conformer using chloroform solvation. ^1H and ^{13}C chemical shifts for each conformer were computed at the WP04, WC04, B3LYP, and PBE1 density functional levels as Boltzmann averages of IEFPCM/B3LYP/6-311+G(2d,p) energies over each family. Comparisons between experimental and theoretical chemical shift data were made using the total absolute error ($|\Delta\delta|_{\text{T}}$) criterion. For the ^1H shift data, all methods were sufficiently accurate to identify the proper stereoisomers. Computed ^{13}C shifts were not always successful in identifying the correct stereoisomer, regardless of which DFT method was used. The relative ability of each theoretical approach to discriminate among stereoisomers on the basis of proton shifts was also evaluated. Copyright © 2007 John Wiley & Sons, Ltd.

Supplementary electronic material for this paper is available in Wiley InterScience at <http://www.interscience.wiley.com/jpages/0749-1581/suppmat/>

KEYWORDS: NMR; ^1H ; ^{13}C ; computed *versus* experimental shifts; diastereomers; penams

INTRODUCTION

The use of *ab initio* calculations to support the interpretation and assignment of NMR spectra has become very prevalent in recent years. In the last decade, ^1H and ^{13}C chemical shifts of organic molecules have frequently been computed using density functional theory (DFT) and other approaches.^{1–15} Such calculations can provide a crucial link between structural and stereochemical details and the corresponding empirical NMR chemical shifts.^{16–29} For molecules of moderate to large size, DFT offers the most economical combination of accuracy and efficiency amongst quantum chemical models, and a number of functionals for the prediction of chemical shift values have been evaluated.³⁰

Accurate computation of NMR chemical shifts using DFT requires some attention to technical detail. In general, modern functionals with large basis sets provide results of reasonable quantitative accuracy.³¹ Accuracy can be improved by the use of DFT methods empirically optimized

for the computation of chemical shifts, or the use of linear regression approaches to correct systematic errors associated with smaller basis sets and/or inaccurate functionals.^{32–38}

Application of these approaches to stereochemical problems, including those involving issues of relative configuration,³⁹ significantly extends their practical value. In order to distinguish among stereoisomers, it is imperative that correct experimental chemical shifts first be in hand. Fortunately, the assignment of chemical shifts, even in quite complex natural structures (e.g., natural products) has become more routine, given recourse to coupling data,⁴⁰ increasingly high-field magnets, novel pulse sequences, and multidimensional NMR experiments.⁴¹ It is worth noting that one need not have 100% of the resonances assigned (although they happen to be for 1–4 and 6–8); rather, it is only essential that 100% of the portion of resonances that are assigned (best when that portion is large) be done so with 100% certainty.

An open question with respect to a computed chemical shifts is whether a given method is sufficiently accurate to capture the magnetic effects associated with stereochemical differences. High accuracy is required for definitive stereochemical assignment, particularly in cases where not all of

*Correspondence to: Thomas R. Hoye, Department of Chemistry, University of Minnesota, 207 Pleasant St. SE, Minneapolis, MN 55455-0431, USA. E-mail: hoye@chem.umn.edu

the stereoisomers may be available for comparison against one another. So, when complete or nearly complete sets of such stereoisomers *are* available, they can serve as useful benchmarks for evaluation, and this work addresses a particular case in point.

The penam β -lactams **1** through **4** (esters) and **5** through **8** (acids) shown in Fig. 1 were chosen as substrates to test the ability of the B3LYP,^{42–45} PBE1,^{46,47} WP04,³² and WC04³² density functional models to distinguish each of the four stereoisomers using experimental and theoretical chemical shift data. The statistical criteria used were total absolute error ($|\Delta\delta|_T$), mean unsigned error (MUE), and mismatch to match ratios of $|\Delta\delta|_T$.

Penam β -lactams contain a challenging variety of functional groups and chemical bonding situations. While some of **1–8** have been previously prepared and reported in the literature,^{48,49} we independently synthesized the full complement of stereoisomers (except for **5**, which did not prove to be stable in our hands) to most meaningfully evaluate various computational approaches. We used, primarily, the methods of Kukulja,⁵⁰ Schofield,⁴⁹ and Fisher and Trinkle⁵¹ to prepare these compounds. The ¹H and ¹³C NMR chemical shifts for each compound were then fully assigned using 1D, 2D, and NOE NMR experiments, with guidance from existing NMR analyses in the penam family. The details supporting those assignments are presented next; readers more interested in the computational aspects are directed to the section 'Computational Methods' further below.

NMR CHEMICAL SHIFT ASSIGNMENTS

For all compounds (**1–4**, **6–8**) the aromatic (phthaloyl), methyl ester, carboxylic acid, and gem-dimethyl protons

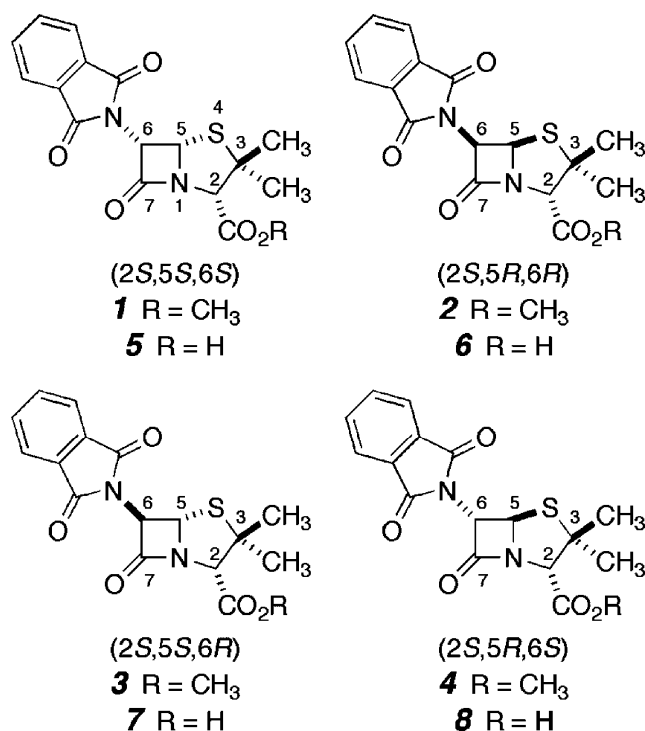


Figure 1. Structures and configurations of the β -lactams investigated in this study.

were straightforward to assign. Protons H-2, H-5, and H-6 and their α (down and *cis* to the carboxyl) or β (up and *trans* to the carboxyl) orientations were assigned on the basis of a combination of HMQC, long-range ¹H–¹H coupling, and/or NOE experiments, as detailed below for each case. Carbon chemical shifts were assigned on the bases of the HMQC and HMBC analyses. In addition, one-bond ¹H–¹³C coupling values were useful for distinguishing C-5 and C-6 (as previously observed for similar penam derivatives⁵²)—all of the ¹J_{C–H–6} values fell in the range of 148–168 Hz while the ¹J_{C–H–5} values were all between 174 and 182 Hz. Two- and three-bond ¹H–¹³C coupling distinguished the three types of carbonyl resonances present in each spectrum: (i) the phthaloyl carbonyl carbons were coupled to H-6 but not H-5 for each compound, (ii) the ester carbonyl resonance (in **1–4**) included a quartet from coupling to the methyl group, (iii) the ester and acid (**6–8**) carbonyl carbon resonances all showed a doublet from coupling to H-2 and (iv) the lactam carbonyl was coupled to H-2, H-5, and H-6. In the following discussion, the preparation of each compound (**1–4**, **6–8**) is briefly summarized, and specific, noteworthy spectral features that support the shift assignments are presented.

The (2*S*, 5*S*, 6*S*)-penam methyl esters **1** and **4** were prepared starting from (2*S*, 5*R*, 6*R*)-6-aminopenicillanic acid (6-APA, Aldrich). The 6-APA was phthaloylated (*N*-carbethoxyphthalimide), esterified (MeI, K₂CO₃, DMF, rt), and base epimerized (DBU, CH₂Cl₂, rt) at C-6 to give the methyl ester **4** (100% *trans* isomer). Subsequent epimerization of the thiazolidine ring at C-5 was achieved by use of the Kukulja procedure⁵⁰ (Cl₂, CCl₄ or CH₂Cl₂, rt; SnCl₄, THF, rt), through which oxidative cleavage of the sulfide and reductive reclosure gave a mixture (1.8:1) of **4** (major) and **1** (minor). These were separated by silica gel column chromatography.

The ¹H NMR resonances for H-2, H-5, and H-6 in the spectrum of **1** were assigned using coupling constant analysis, NOE, and HMQC experiments. The value of the coupling constant between the H-6 (5.63 ppm) and H-5 (5.29 ppm) protons ($J = 4.2$ Hz) was consistent with their *cis* orientation on the lactam ring.⁵³ The β -oriented H-2 resonance (4.00 ppm) showed an NOE to the singlet at 1.71 ppm, which was therefore assigned as the protons from the β -methyl group, and not to that at 1.73 ppm, which was assigned to the α -methyl protons.

In the proton-coupled ¹³C NMR spectrum of **1** the phthalimido carbonyl carbon at 166.8 ppm appeared as a dd ($J = 4, 4$ Hz) due to the couplings with H-6 and a phthalimido *ortho*-proton; the ester carbonyl carbon at 165.7 ppm displayed coupling to H-2 and the ester methyl group and appeared as a dq ($J = 8, 4$ Hz); the lactam carbonyl carbon (C-7, 165.3) appeared as a ddd due to coupling with H-2 ($J = 10$ Hz), H-5 ($J = 7$ Hz), and H-6 ($J = 7$ Hz). Each of the C-5 and C-6 resonances at 63.6 and 59.1 ppm, respectively, was a dd ($J = 174, 4$ Hz and $J = 149, 4$ Hz, respectively); these observations are consistent with earlier observations made for similar penicillin derivatives.⁵²

The (2*S*, 5*R*, 6*R*)-penam methyl ester **2** was prepared by phthaloylation and esterification of 6-APA, retaining the original (2*S*, 5*R*, 6*R*)-configuration. The J value of 4.1 Hz

between the H-6 and H-5 protons at 5.68 and 5.61 ppm, respectively, confirmed their *cis* arrangement on the lactam ring. Again, an NOE experiment involving irradiation of the H-2 β -methine singlet (at 4.68 ppm) allowed the assignment of the β - versus the α -methyl group resonances at 1.83 and 1.51 ppm, respectively.

In the proton-coupled ^{13}C NMR spectrum of **2** the phthalimido carbonyl carbon at 166.8 ppm again appeared as a dd ($J = 3, 3$ Hz) due to coupling with the H-6 and the *ortho* phthalimido protons. The ester and lactam (C-7) carbonyl resonances appeared as overlapping multiplets centered at 168.6 ppm. The C-5 resonance at 67.1 appeared as a ddd ($J = 176, 4, 3$ Hz) from coupling to H-5, H-6, and H-2, respectively, while the C-6 resonance at 58.6 ppm was a dd ($J = 150, 3$ Hz) from coupling to H-6 and H-5.

The (2*S*, 5*S*, 6*R*)-penam methyl ester **3** was prepared by phthaloylation and esterification of 6-APA followed by Kukolja epimerization at C-5, which gave a mixture (7.4:1) of **3** (major) and **2** (minor). These were separated by silica gel column chromatography. The J value of 2.3 Hz between the H-6 and H-5 resonances at 5.56 and 5.44 ppm indicate that these protons have a *trans* orientation on the lactam ring. Irradiation of the H-2 β -methine proton at 3.90 ppm leads to an NOE enhancement of the C-3 β -methyl resonance at 1.69 ppm. By default, the C-3 α -methyl group was at 1.49 ppm.

In the proton-coupled ^{13}C NMR spectrum, of **3** the phthalimido carbonyl carbon at 166.8 ppm again appeared as a dd ($J = 4$ and 4 Hz) due to coupling with the H-6 and the *ortho* phthalimido protons. The ester carbonyl at 167.3 ppm was a dq ($J = 4$ and 4 Hz) arising from coupling to H-2 and the methoxy protons. The lactam (C-7) carbonyl carbon at 165.9 ppm was a ddd ($J = 7, 3,$ and 2 Hz), due to coupling with H-2, H-5, and H-6, respectively. As with **1** and **2**, the C-5 resonance at 66.6 ppm was a ddd ($J = 177, 4,$ and 4 Hz) and C-6 at 60.1 ppm a d ($J = 152$ Hz).

In the ^1H NMR spectrum of the (2*S*, 5*R*, 6*S*)-penam methyl ester **4**, the H-5 to H-6 J value of 1.8 Hz (at 5.58 and 5.41 ppm, respectively) indicated their *trans* orientation on the lactam ring. Irradiation of the H-2 methine proton produced a NOE enhancement of the C-3 β -methyl singlet at 1.66 ppm. By default the C-3 α -methyl group singlet resided at 1.49 ppm.

In the proton-coupled ^{13}C NMR spectrum the phthalimido carbonyl carbon at 166.6 ppm appeared as a dd ($J = 4, 4$ Hz) due to the couplings with the H-6 and the *ortho* phthalimido protons. The ester carbonyl carbon at 167.8 ppm displayed coupling to H-2 and the ester methyl group and appeared as a dq ($J = 5, 4$ Hz). The lactam carbonyl carbon (C-7, 167.4 ppm) was a ddd ($J = 6, 4,$ and 4 Hz) due to the coupling with H-2, H-5, and H-6, respectively. The C-5 resonance (69.2 ppm) was a ddd ($J = 178, 7, 4$ Hz) and C-6 (64.5 ppm) a d ($J = 152$ Hz).

We then attempted to prepare the entire set of stereoisomeric carboxylic acids **5** through **8** from the corresponding methyl esters **1** through **4** by the ester cleavage methodology of Fisher and Trinkle (LiI, EtOAc, reflux).⁵¹ This was successful for **6**–**8**, but failed in the case of **5**. Imine **9** (Fig. 2(a)), the enantiomer of which was previously prepared by Schutz

and Ugi⁵⁴ and then Baldwin *et al.*⁵⁵ using different methods, was formed instead.

The ^1H and ^{13}C NMR shift assignments for acids **6** through **8** were made using similar analyses to those detailed above for esters **1** through **4**. Other than the small differences in the values themselves, the chemical shift trends among sets of related compounds were maintained. Of course, for each the resonance for the carboxyl carbon in the proton-coupled ^{13}C NMR spectrum now appeared just as a doublet (rather than a dq) because of coupling only to H-2.

COMPUTATIONAL METHODS

Each β -lactam was modeled as a family of conformers characterized by different dihedral angles about the C-6–N, the ester C-2–C bond, and the ester C–O bonds. By varying the torsional angles about the N-1–C-7, C-3–S-4, and C-5–S-4 bonds, the conformations of the thiazolidine ring⁵⁶ were also considered (i.e. the C-3 envelope and the S-4 envelope forms). Conformer families were obtained from Monte Carlo conformational searches (50 000 steps; the degrees of freedom are illustrated in Fig. 2(b)) and geometry optimization with PRCG^{57,58} (500 steps). The force field AMBER^{59,60} (as implemented in Macromodel 6.0) and the GB/SA solvation model⁶¹ for chloroform were used throughout the study.

All the minimum energy conformer geometries obtained were then fully optimized at the density functional level of theory employing the hybrid generalized gradient approximation (GGA) functional B3LYP^{42–45} with the 6-31G(d) basis set.⁶² Chloroform solvation effects were included via the integral equation formalism polarized continuum model (IEFPCM).^{63–66} Solute cavities were constructed using default united-atom radii⁶⁶ (UA0).

For each optimized conformer geometry, ^1H and ^{13}C atomic chemical shielding tensors σ were computed³⁰ at the density functional level using the gauge independent atomic orbital (GIAO) formalism,^{67–69} the 6-311 + G(2d,p) basis set, and chloroform solvation as modeled by IEFPCM^{70,71} employing solute cavities built from Bondi radii.⁷² Isotropic atomic chemical shifts (δ) in units of ppm were computed as differences between the atomic isotropic shieldings of

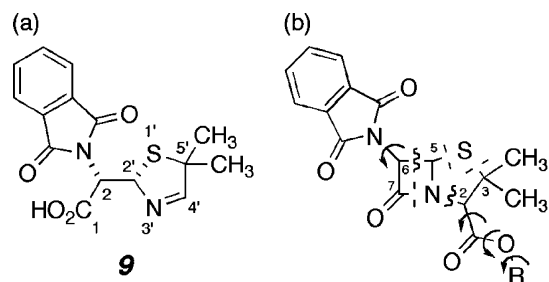


Figure 2. (a) Imine **9**, byproduct formed during attempted synthesis of acid **5** from ester **1**. (b) Degrees of freedom surveyed by Monte Carlo conformational searches. Arrows indicate viable rotations, dotted lines torsion sites, and wavy lines ring-closure sites.

the solutes and corresponding reference atoms in tetramethylsilane (TMS). Four hybrid GGA functionals were examined – namely, B3LYP,^{42–45} PBE1,^{46,47} WP04,³² and WC04.³² Population-averaged chemical shifts for each family of conformers were computed assuming Boltzmann statistics based on B3LYP/6-311 + g(2d,p) free energies including chloroform solvation effects according to^{20,31}

$$\delta = \sum_i \left(\frac{\delta_i e^{-G_i^0/RT}}{\sum_j e^{-G_j^0/RT}} \right) \quad (1)$$

where i and j run over conformers, G is the free energy of the conformer in solution, R is the universal gas constant, and T is 298 K. The free energy in solution is taken as the sum of the electronic energy and solvation free energy computed at the B3LYP level using the 6-311 + G(2d,p) basis set⁶² and IEFPCM chloroform solvation free energies.

The specific numbers of conformers in each family used for modeling were 12 for **1**, 10 for **2**, 12 for **3**, 12 for **4**, 14 for **6**, 16 for **7**, and 16 for **8**. For the penam methyl esters **1–4**, 16 protons and 17 carbons were modeled while 13 protons and 16 carbons were modeled for the penams **5–8**. The computed ¹H shifts of each methyl group were arithmetically averaged owing to their free rotation at 298 K. The ¹H and ¹³C shifts of the corresponding *ortho*, *para*, and *ipso* positions of the phthalimido group were averaged during the Boltzmann process. A pruned (75, 302) integration grid containing 75 radial shells and 302 angular points per shell (approximately 7000 points for each atom) was used on each atom. Density functional calculations were carried out using the Gaussian 03 suite of electronic structure programs.⁷³

RESULTS AND DISCUSSION

Linear correction of computed chemical shifts

Linear corrections of computed chemical shifts have been found to be useful for correcting systematic errors associated with particular density functionals and thereby improving the accuracy of their predictions.^{32–38} In particular, the linear corrections listed in Table 1, which were optimized over a diverse training set of small molecules not including the penams,³² were applied to the ¹H and ¹³C chemical shift values (δ^{comp}) obtained with each of the functionals we studied; corrected predictions (δ^{corr}) are determined according to:

$$\delta^{\text{corr}} = m \times \delta^{\text{comp}} + b \quad (2)$$

where m is the slope and b the intercept specific to a particular functional/basis set combination.

Criteria for evaluating DFT methods

Methods were evaluated for their ability to make stereochemical distinctions using the following statistical parameters: the absolute error between computed and experimental chemical shifts ($|\Delta\delta|_T$, ppm)

$$|\Delta\delta|_T = \sum_i |\delta_i^{\text{corr}} - \delta_i^{\text{exp}}| \quad (3)$$

the MUE between computed and experimental shifts (MUE, ppm)

$$MUE = \sum_i |\delta_i^{\text{corr}} - \delta_i^{\text{exp}}| / n \quad (4)$$

where n is the total number of chemical shifts under consideration; and the ratio of the total absolute error for all of the stereochemical mismatches to the total absolute error of the stereochemical matches (Eqn 5).

$$R = \left(\sum_j |\Delta\delta|_T^{\text{miss}} \right) / |\Delta\delta|_T^{\text{match}} \quad (5)$$

Use of relative configuration of penam methyl esters to evaluate computed ¹H NMR chemical shifts

We have previously assessed the influence of stereochemistry on proton and carbon chemical shifts for a series of monomethylcyclohexanols using small families of conformers.⁷⁴ The studies presented here extend that methodology to larger molecules containing multiple stereogenic centers and a much wider array of functionality and heteroatoms. Monte Carlo conformational searches followed by geometry optimization using the AMBER* force field is an efficient approach to construct conformer families in the penams. Because of the approximate nature of the force field and its associated parameters, particularly with respect to potentially challenging combinations of functional groups like those present in penams **1–8**, we subsequently reoptimized all conformer geometries at the IEFPCM/B3LYP/6-31G(d) level of theory.

The ¹H NMR chemical shifts were computed using the B3LYP, PBE1, and WP04 methods described previously. Various combinations of experimental and theoretically computed chemical shifts data were evaluated using the total absolute error ($|\Delta\delta|_T$) criterion. The best correlation (smallest $|\Delta\delta|_T$ value) was used to identify a configurational match. The correlation data for penams **1–4** is summarized in Tables 2–4. For example, in Table 2 the experimental shift data for **1** (1^{exp}) are correlated with the computed shifts for each of **1–4** ($1^{\text{corr}}\text{–}4^{\text{corr}}$). The total absolute error is best (smaller) for the matched pair 1^{exp} versus 1^{corr} and poorer

Table 1. Slope (m , unitless) and intercept (b , ppm) values for linear correction of chemical shifts³² for various density functionals^a

Theory	¹³ C		¹ H	
	m	b	m	b
B3LYP	0.9488	–2.1134	0.9333	0.1203
WP04	0.9601	–3.0273	0.9587	0.1127
WC04	1.0032	–0.9647	0.9451	0.1157
PBE1	0.9486	–1.257	0.9169	0.1895

^a For use with IEFPCM/Theory/6-311 + G(2d,p) // IEFPCM/B3LYP/6-31G(d).

Table 2. Correlation data for methyl penams 1–4 using IEFPCM/B3LYP/6-311+G(2d,p)//IEFPCM/B3LYP/6-31G(d) and experimental ^1H NMR chemical shifts^a

	1^{corr}	2^{corr}	3^{corr}	4^{corr}
1^{exp}	1.21	2.67	2.20	2.89
2^{exp}	2.12	0.86	3.33	1.86
3^{exp}	1.89	3.07	0.94	2.66
4^{exp}	2.24	1.36	2.54	0.96

^a $|\Delta\delta|_{\text{T}}$ values reported in ppm.**Table 3.** Correlation data for methyl penams 1–4 using IEFPCM/PBE1/6-311 + G(2d,p)//IEFPCM/B3LYP/6-31G(d) and experimental ^1H NMR chemical shifts^a

	1^{corr}	2^{corr}	3^{corr}	4^{corr}
1^{exp}	1.21	2.78	1.96	2.64
2^{exp}	2.16	0.90	3.30	1.66
3^{exp}	2.01	3.18	0.94	2.55
4^{exp}	2.38	1.42	2.47	0.83

^a $|\Delta\delta|_{\text{T}}$ values reported in ppm.**Table 4.** Correlation data for methyl penams 1–4 using IEFPCM/WP04/6-311 + G(2d,p)//IEFPCM/B3LYP/6-31G(d) and experimental ^1H NMR chemical shifts^a

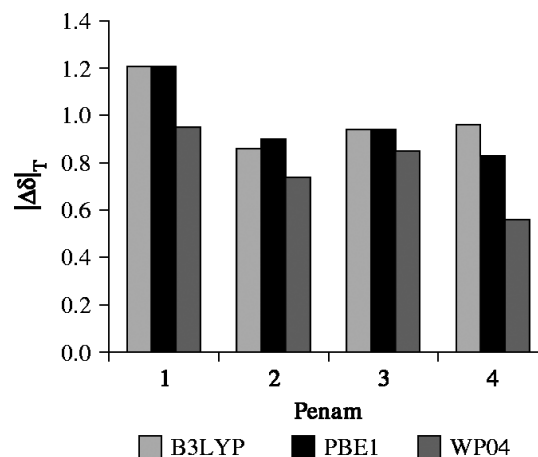
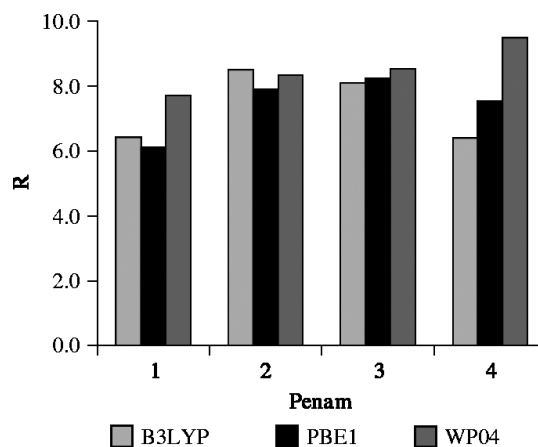
	1^{corr}	2^{corr}	3^{corr}	4^{corr}
1^{exp}	0.95	2.60	1.93	2.80
2^{exp}	1.88	0.74	2.83	1.46
3^{exp}	1.74	3.07	0.85	2.45
4^{exp}	1.98	1.14	2.19	0.56

^a $|\Delta\delta|_{\text{T}}$ values reported in ppm.

(larger) for all other pairs (~2 times larger for mismatched pairs vs the correct pair).

In general, the data in Tables 2–4 indicate that each of the B3LYP, PBE1, and WP04 methods (with chloroform solvation effects included) were able to distinguish convincingly amongst all configurations. By considering the diagonal sums of the $|\Delta\delta|_{\text{T}}$ values (boldface in tables) or the corresponding MUE, WP04 computed chemical shifts are more accurate than those of B3LYP and PBE1 for penams 1–4. The $|\Delta\delta|_{\text{T}}$ sums for each method were 3.97 ppm for B3LYP, 3.88 ppm for PBE1, and 3.10 ppm for WP04 (~20% lower than PBE1). The diagonal $|\Delta\delta|_{\text{T}}$ data from Tables 2–4 are also combined and displayed graphically in Fig. 3. For each method, the MUE of the correct matches was 0.06 ppm for B3LYP, 0.06 ppm for PBE1, and a slightly better 0.05 ppm for WP04.

The relative ability of a theoretical method to distinguish between configurations can be judged by comparing R -ratios, the mismatch to match ratios of $|\Delta\delta|_{\text{T}}$. The R -ratios for each of the penams 1–4 using each of three DFT methods are displayed in Fig. 4. A larger value of R indicates a greater ability to discriminate the matched from the mismatched diastereomers. For 1–4 WP04 has, on average, R -ratios that are 14 and 16% larger than those using PBE1 and B3LYP, respectively.

**Figure 3.** Graphical representation of total absolute error ($|\Delta\delta|_{\text{T}}$) data for penam esters 1–4 using the indicated theoretical method.**Figure 4.** Graphical representation of R -ratios for penam esters 1–4 using the indicated theoretical method.

Use of the relative configuration of penam carboxylic acids to evaluate computed ^1H NMR chemical shifts

Tables 5–7 list the $|\Delta\delta|_{\text{T}}$ values from the various correlations of experimental ^1H shifts obtained for acids 6–8 to those computed at the B3LYP, PBE1, and WP04 levels for penams 5–8. Again, each method was successfully able to make stereochemical distinctions between all cases using the $|\Delta\delta|_{\text{T}}$ criterion. However, this time the diagonal sums of the $|\Delta\delta|_{\text{T}}$ values (emboldened matches) and the corresponding MUEs indicate that PBE1 computed chemical shifts are more accurate than those of B3LYP and WP04 for penams 6–8. The $|\Delta\delta|_{\text{T}}$ sums for each method was 2.48 ppm for B3LYP, 2.22 ppm for WP04, and 1.84 ppm for PBE1 (~17% lower than WP04). The diagonal $|\Delta\delta|_{\text{T}}$ data of Tables 5–7 are also displayed graphically in Fig. 5. For each method, the MUE of the correct matches was 0.06 ppm for B3LYP, 0.06 ppm for WP04, and 0.05 ppm for PBE1.

The R -ratios for the proton chemical shifts for penam acids 6–8, again using each of three DFT methods, appear in Fig. 6. On average, the PBE1 R -ratios are 16 and 25% larger (better) than those of WP04 and B3LYP, respectively.

Table 5. Correlation data for penams 6–8 using IEFPCM/B3LYP/6-311+G(2d,p)//IEFPCM/B3LYP/6-31G(d) and experimental ^1H NMR chemical shifts^a

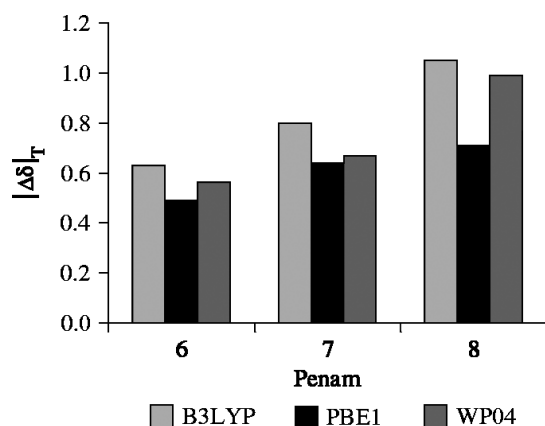
	5 ^{corr}	6 ^{corr}	7 ^{corr}	8 ^{corr}
6 ^{exp}	1.80	0.63	2.86	1.64
7 ^{exp}	1.16	2.49	0.80	2.16
8 ^{exp}	1.92	1.10	2.04	1.05

^a $|\Delta\delta|_{\text{T}}$ values reported in ppm.**Table 6.** Correlation data for penams 6–8 using IEFPCM/PBE1/6-311+G(2d,p)//IEFPCM/B3LYP/6-31G(d) and experimental ^1H NMR chemical shifts^a

	5 ^{corr}	6 ^{corr}	7 ^{corr}	8 ^{corr}
6 ^{exp}	1.81	0.49	2.73	1.31
7 ^{exp}	1.25	2.32	0.64	1.92
8 ^{exp}	2.07	1.03	1.91	0.71

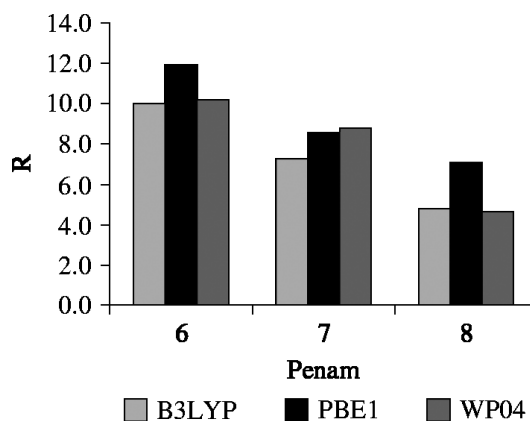
^a $|\Delta\delta|_{\text{T}}$ values reported in ppm.**Table 7.** Correlation data for penams 6–8 using IEFPCM/WP04/6-311+G(2d,p)//IEFPCM/B3LYP/6-31G(d) and experimental ^1H NMR chemical shifts^a

	5 ^{corr}	6 ^{corr}	7 ^{corr}	8 ^{corr}
6 ^{exp}	1.62	0.56	2.52	1.57
7 ^{exp}	1.16	2.59	0.67	2.15
8 ^{exp}	1.76	1.12	1.73	0.99

^a $|\Delta\delta|_{\text{T}}$ values reported in ppm.**Figure 5.** Graphical representation of total absolute error ($|\Delta\delta|_{\text{T}}$) data for penam acids 6–8 using the indicated theoretical method.

Overall evaluation of methods for computing ^1H NMR chemical shifts

The average R -ratios across the sets of penams 1–4, 6–8, and the combined sets 1–4 and 6–8 are displayed in Fig. 7. For both the penam esters (1–4) and acids (6–8), the popular B3LYP method does not perform as well as PBE1 or WP04 in its ability to discriminate among stereoisomers. For the penam esters 1–4, WP04 outperforms B3LYP and PBE1,

**Figure 6.** Graphical representation of R -ratios for penam esters 6–8 using the indicated theoretical method.

while for the acids 6–8, PBE1 outperforms B3LYP and WP04. Averaging the R -ratios across both sets of penams indicates that WP04 and PBE1 are best and nearly equivalent.

Use of the relative configuration of penam methyl esters to evaluate computed ^{13}C NMR chemical shifts

We also examined additional correlations for 1–4 by comparing the B3LYP, PBE1, and WC04 predictions for carbon chemical shifts with experiment using the same statistical criterion ($|\Delta\delta|_{\text{T}}$) described above. The data in Table 8 indicate that the widely employed B3LYP model fails to identify the proper isomer in two of four cases: ($|\Delta\delta|_{\text{T}}$) is minimized for the incorrect match of 2^{exp} with 1^{corr} as well as 3^{exp} with 1^{corr}.

The ^{13}C shift comparisons using the PBE1 and WC04 models are summarized in Tables 9 and 10. Like the B3LYP model, neither PBE1 nor WC04 successfully distinguishes 1, 2, and 3 from one another. The failure of each of the methods indicates that assigning stereochemistry using ^{13}C shifts computed by any of these methods is unwise.

For the B3LYP and PBE1 methods the largest contributions to the shift error are associated with the C-3 and C-5 atoms (i.e. two of the 17 carbons in each compound): 26.1% of the error is due to C-3 and 12.5% to C-5. WC04 also had

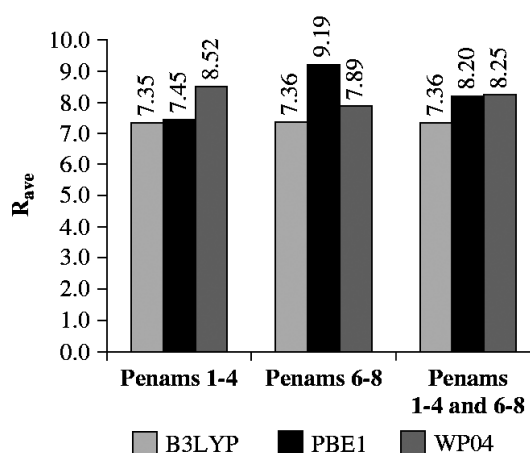
**Figure 7.** Comparison of average R -ratios for penam esters 1–4 and acids 6–8 using the indicated theoretical method.

Table 8. Correlation data for methyl penams **1–4** using IEFPCM/B3LYP/6-311+G(2d,p)//IEFPCM/B3LYP/6-31G(d) and experimental ^{13}C NMR chemical shifts^a

	1 ^{corr}	2 ^{corr}	3 ^{corr}	4 ^{corr}
1 ^{exp}	38.3	51.2	45.9	60.4
2 ^{exp}	35.8	37.2	44.6	45.2
3 ^{exp}	32.1	47.8	35.8	54.8
4 ^{exp}	48.3	45.1	52.7	37.0

^a $|\Delta\delta|_{\text{T}}$ values reported in ppm.**Table 9.** Correlation data for methyl penams **1–4** using IEFPCM/PBE1/6-311+G(2d,p)//IEFPCM/B3LYP/6-31G(d) and experimental ^{13}C NMR chemical shifts^a

	1 ^{corr}	2 ^{corr}	3 ^{corr}	4 ^{corr}
1 ^{exp}	32.6	47.8	40.7	55.2
2 ^{exp}	31.8	34.4	41.8	41.7
3 ^{exp}	27.6	44.3	33.0	49.6
4 ^{exp}	46.5	40.6	48.4	34.5

^a $|\Delta\delta|_{\text{T}}$ reported in ppm.**Table 10.** Correlation data for methyl penams **1–4** using IEFPCM/WC04/6-311+G(2d,p)//IEFPCM/B3LYP/6-31G(d) and experimental ^{13}C NMR chemical shifts^a

	1 ^{corr}	2 ^{corr}	3 ^{corr}	4 ^{corr}
1 ^{exp}	60.8	64.6	60.4	65.3
2 ^{exp}	59.7	57.3	61.7	54.3
3 ^{exp}	60.1	68.6	59.8	67.9
4 ^{exp}	73.1	67.7	75.1	59.3

^a $|\Delta\delta|_{\text{T}}$ reported in ppm.

somewhat larger average errors for these atoms (7.9% on C-3 and 7.1% on C-5) but exhibited significant error on other atoms as well, such as C-7 (11.2%), C-2 (14.6%), C-6 (9.1%), and the ester carbonyl (8.2%). The proximity of C-3 and C-5 to the attached sulfur atom and the consistently too large (PBE1, B3LYP) or too small (WC04) computed ^{13}C shifts for these atoms suggest that the modeling may be failing to account for subtle features in the carbon sulfur bonds, even though dimethyl sulfide was included in the WC04 training set.³²

Use of the relative configuration of penam carboxylic acids to evaluate computed ^{13}C NMR chemical shifts

Correlation data for compounds **5–8** are presented in Tables 11–13. The data in Tables 11 and 12 indicate that the B3LYP and PBE1 methods are able to distinguish between all available isomers for this set, although computed errors continue to be dominated at the C-3 (26.6%) and C-5 (12.6%) atoms. WC04, on the other hand, fails to distinguish **6**^{exp} from **8**^{corr} (Table 13).

Within this set of penam acid isomers (**5–8**), the B3LYP methods and PBE1 appeared to perform satisfactorily for the prediction of relative configuration based on ^{13}C chemical

Table 11. Correlation data for penams **6–8** using IEFPCM/B3LYP/6-311+G(2d,p)//IEFPCM/B3LYP/6-31G(d) and experimental ^{13}C NMR chemical shifts^a

	5 ^{corr}	6 ^{corr}	7 ^{corr}	8 ^{corr}
6 ^{exp}	46.2	37.0	43.9	47.1
7 ^{exp}	41.7	43.1	35.6	50.2
8 ^{exp}	60.4	42.6	48.8	36.9

^a $|\Delta\delta|_{\text{T}}$ values reported in ppm.**Table 12.** Correlation data for penams **6–8** using IEFPCM/PBE1/6-311+G(2d,p)//IEFPCM/B3LYP/6-31G(d) and experimental ^{13}C NMR chemical shifts^a

	5 ^{corr}	6 ^{corr}	7 ^{corr}	8 ^{corr}
6 ^{exp}	42.2	35.0	38.6	44.8
7 ^{exp}	37.6	40.8	30.1	46.7
8 ^{exp}	58.1	39.1	44.8	35.8

^a $|\Delta\delta|_{\text{T}}$ values reported in ppm.**Table 13.** Correlation data for penams **6–8** using IEFPCM/WC04/6-311+G(2d,p)//IEFPCM/B3LYP/6-31G(d) and experimental ^{13}C NMR chemical shifts^a

	5 ^{corr}	6 ^{corr}	7 ^{corr}	8 ^{corr}
6 ^{exp}	56.0	50.1	51.8	46.0
7 ^{exp}	55.1	61.0	52.7	58.8
8 ^{exp}	68.2	60.5	62.6	51.1

^a $|\Delta\delta|_{\text{T}}$ values reported in ppm.

shift comparison. However, this success is mitigated by the failure of these same methods to correctly predict the stereochemistry of penam ester isomers **1–4** using ^{13}C shifts. This outcome significantly contrasts the use of ^1H chemical shifts and suggests that the latter are of greater utility for drawing stereochemical distinctions.

Evaluating the use of only the global minimum energy conformer

In Table 14 are listed the relative conformer energies and percentages of the families used to model methyl penams **1–4**. For each, the global minimum conformer comprises 37–68% of the total conformational population. For the purpose of possible simplification, we examined the merit of using only those ^1H chemical shifts computed for the global minimum energy conformer to distinguish among the diastereomers.

Statistical data for the WP04 ^1H NMR chemical shifts are provided in Table 15. All stereochemical distinctions are made successfully using only the data of the global minimum conformer. Indeed, the accuracy is unchanged considering the MUE value for stereochemical matches (0.05 ppm, Table 15) compared to the MUE obtained using the full complement of conformers (0.05 ppm, Table 4). The *R*-ratio did degrade somewhat going from 8.52 for the full conformer complement to 8.40.

An appealing idea is that the use of the global minimum energy conformer may not be necessary, but that *any* single

Table 14. Relative energies and percentages of conformers used to model the penam methyl esters **1–4**^a

Conf	1		2		3		4	
	ΔG	%						
<i>a</i>	0.0	68	0.0	37	0.0	55	0.0	55
<i>b</i>	0.9	16	0.2	27	0.4	29	0.3	30
<i>c</i>	1.1	11	0.3	21	0.9	12	1.1	8
<i>d</i>	1.7	4	0.6	14	1.9	2	1.2	8
<i>e</i>	2.2	1	7.6	0	2.5	1	7.8	0
<i>f</i>	10.9	0			8.0	0	9.6	0

^a ΔG values are relative energies (kcal mol⁻¹) above the global minimum (boldface) computed using IEFPCM/B3LYP/6-311+G(2d,p).

Table 15. Single conformer correlation data for methyl penams **1–4** between IEFPCM/WP04/6-311+G(2d,p)//IEFPCM/B3LYP/6-31G(d) and experimental ¹H NMR chemical shifts^a

	1 ^{corr}	2 ^{corr}	3 ^{corr}	4 ^{corr}
1 ^{exp}	1.17	2.87	1.88	3.02
2 ^{exp}	1.79	0.64	2.69	1.47
3 ^{exp}	1.98	3.34	0.80	2.55
4 ^{exp}	2.20	1.14	2.22	0.71

^a $|\Delta\delta|_T$ values reported in ppm.

conformer of the family might be sufficient. This approach will only be useful if the chemical shift differences between each configuration for all permutations are always greater than those caused by common conformational changes. It is unlikely, though, that this will always/often be the case. For example, Table 16 shows correlation data for **1–4** using chemical shifts computed with the WP04 protocol and the conformers *c1*, *d2*, *e3*, and *e4* (Table 14). These conformers produced the worse case scenario of using a single random conformer representation for stereochemical distinction. As is seen in Table 16 the computations now fail to correctly distinguish the relative configurations of **3** and **4** (compare to Tables 4 and 16). The *R*-ratio is also reduced considerably from 8.52 (full complement) to a value of 4.79. The value of Boltzmann averaging chemical shifts across a family of conformers is apparent.

Table 16. Worse-case single conformer correlation data for methyl penams **1–4** between IEFPCM/WP04/6-311+G(2d,p)//IEFPCM/B3LYP/6-31G(d) and experimental ¹H NMR chemical shifts^a

	1 ^{corr}	2 ^{corr}	3 ^{corr}	4 ^{corr}
1 ^{exp}	1.07	2.36	1.77	2.49
2 ^{exp}	2.53	1.26	2.88	1.78
3 ^{exp}	0.91	2.57	1.75	2.61
4 ^{exp}	1.78	0.87	2.10	1.25

^a $|\Delta\delta|_T$ values reported in ppm.

CONCLUSIONS

The approach that provided the most reliable stereochemical assignment of isomeric penam β -lactam derivatives used proton chemical shifts and a Boltzmann-averaged family of conformations whose energies were determined at the B3LYP/6-311+G(2d,p) level including chloroform solvation. The less rigorous approach of using only the global minimum energy geometry also provided correct answers and may be considered for cases where molecular size dictates recourse to this approximation. Among the DFT functionals that were examined for computing the ¹H shifts, each of B3LYP, PBE1, and WP04 was capable of verifying all of the proper diastereomeric correlations. Further evaluation using the *R*-ratio criterion indicated that PBE1 and WP04 performed comparably to one another and somewhat better than B3LYP for stereochemical distinction.

By comparing ¹H NMR chemical shifts with those computed by DFT, it is feasible to deduce the relative configuration of an unknown compound having moderately complex (both in size and functionality) constitution. Analogous analyses of ¹³C data proved less successful; for purposes of stereochemical distinction, the ¹H chemical shifts are more reliable than those of carbon because the shift differences between related diastereomers are more likely to be larger than the computational error.

EXPERIMENTAL

For NMR measurements the sample concentration was approximately 0.7% by weight in CDCl₃ for the 1D ¹H NMR spectra and 2.5% for all others. The ¹³C and ¹H NMR spectra were obtained at ambient temperature with chemical shifts determined relative to CDCl₃ (δ 77.23 ppm) for ¹³C and TMS (δ 0.00 ppm) for ¹H spectra. Proton spectra were recorded with acquisition times of 2 s and a spectral width of 8000 Hz; coupling constant values are significant to the nearest 0.25 Hz. A Varian VI-500 MHz NMR instrument or Varian VXR-300 MHz NMR instrument was used throughout.

High resolution mass spectrometry (HRMS) was performed using a BioTOF II ESI instrument. The source temperature was set to 150 °C, acceleration voltage was 8500 V, and nitrogen was used as the carrier gas. A mass range of 100–1000 amu was used for the analysis; the resolution of the measurement was 10 000 FWHM.

High pressure liquid chromatography (LC) analysis of each compound reported was performed using an Agilent 1100 Series LC equipped with a 4.6 \times 150 mm Zorbax Eclipse XDB-C₁₈ (5 μ m) column using a programmed mobile phase gradient of 10 mM aqueous ammonium acetate and methanol (5–41% methanol over 10 min, then 41–98% over 6 min, holding at 98% methanol for 6 min). Dual detection with Agilent LC/MSD SL (G1978A) and diode array (254 nm, G1315B) detectors was used. Samples were prepared in acetonitrile (~1 mg/ml) and the injection volume was 5 μ l.

(2*S*, 5*S*, 6*S*)-6-(1,3-dioxoisindolin-2-yl)-3,3-dimethyl-7-oxo-4-thia-1-aza-bicyclo[3.2.0]heptane-2-carboxylic acid methyl ester (**1**)

¹H NMR (CDCl₃) δ 1.71 (s, 3H, β Me), 1.73 (s, 3H, α Me), 3.90 (s, 3H, CO₂CH₃), 4.00 (d, 1H, *J* = 1.0 Hz, H2), 5.29

(d, 1H, $J = 4.2$ Hz, H-5), 5.63 (dd, 1H, $J = 4.2, 0.9$ Hz, H-6), 7.77 (m, 2H, Ar_{meta}), 7.89 (m, 2H, Ar_{ortho}); ¹³C NMR δ 27.4 (qm, $J = 129$ Hz, α Me), 30.4 (qm, $J = 128$ Hz, β Me), 52.8 (q, $J = 148$ Hz, CO₂CH₃), 59.1 (dd, $J = 149$ and 4 Hz, C-6), 63.6 (dd, $J = 174$ and 4 Hz, C-5), 65.1 (br m, C-3), 73.1 (dm, $J = 143$ Hz, C-2), 124.0 (dm, $J = 166$ Hz, Ar_{ortho}), 131.7 (m, Ar_{ipso}), δ 134.7 (dd, $J = 165, 8$ Hz, Ar_{meta}), 165.3 (ddd, $J = 10, 7,$ and 7 Hz, C-7), 165.7 (dq, $J = 8$ and 4 Hz, CO₂CH₃), 166.8 (dd, $J = 4$ and 4 Hz, Ar C=O); HRMS Calcd for C₁₇H₁₆N₂NaO₅S (M + Na) 383.0672, found 383.0656 (−4.2 ppm error); LC ($\lambda = 254$ nm) 19.503 min.

(2S, 5R, 6R)-6-(1,3-dioxoisindolin-2-yl)-3,3-dimethyl-7-oxo-4-thia-1-aza-bicyclo[3.2.0]heptane-2-carboxylic acid methyl ester (2)

¹H NMR (CDCl₃) δ 1.51 (s, 3H, α Me), 1.83 (s, 3H, β Me), 3.81 (s, 3H, CO₂CH₃), 4.68 (s, 1H, H-2), 5.61 (d, 1H, $J = 4.2$ Hz, H-5), 5.68 (d, 1H, $J = 3.9$ Hz, H-6), 7.77 (m, 2H, Ar_{meta}), 7.89 (m, 2H, Ar_{ortho}); ¹³C NMR δ 28.2 (qm, $J = 129$ Hz, α Me), 31.1 (qm, $J = 129$ Hz, β Me), 52.7 (q, $J = 148$ Hz, CO₂CH₃), 58.6 (dd, $J = 150, 3$ Hz, C-6), 66.2 (br m, C-3), 67.1 (ddd, $J = 176, 4, 3$ Hz, C-5), 71.1 (dm, $J = 146$ Hz, C-2), 124 (dm, $J = 166$ Hz, Ar_{ortho}), 131.7 (m, Ar_{ipso}), 134.7 (dd, $J = 164, 7$ Hz, Ar_{meta}), 166.8 (dd, $J = 4, 4$ Hz, Ar C=O), 168.6 (m, CO₂CH₃), 168.6 (m, C-7); HRMS Calcd C₁₇H₁₆N₂NaO₅S for (M + Na) 383.0672, found 383.0666 (−1.6 ppm error); LC ($\lambda = 254$ nm) 19.640 min.

(2S, 5S, 6R)-6-(1,3-dioxoisindolin-2-yl)-3,3-dimethyl-7-oxo-4-thia-1-aza-bicyclo[3.2.0]heptane-2-carboxylic acid methyl ester (3)

¹H NMR (CDCl₃) δ 1.49 (s, 3H, α Me), 1.69 (s, 3H, β Me), 3.84 (s, 3H, CO₂CH₃), 3.90 (s, 1H, H-2), 5.44 (d, 1H, $J = 2.0$ Hz, H-5), 5.56 (d, 1H, $J = 2.5$ Hz, H-6), 7.77 (m, 2H, Ar_{meta}), 7.90 (m, 2H, Ar_{ortho}); ¹³C NMR δ 25.0 (qm, $J = 129$ Hz, α Me), 31.4 (qm, $J = 129$ Hz, β Me), 52.8 (q, $J = 148$ Hz, CO₂CH₃), 60.1 (d, $J = 152$ Hz, C-6), 66.0 (br m, C-3), 66.6 (ddd, $J = 177, 4, 4$ Hz, C-5), 70.5 (dm, $J = 151$ Hz, C-2), 124.1 (dm, $J = 168$ Hz, Ar_{ortho}), 131.8 (m, Ar_{ipso}), 134.8 (dm, $J = 164$ Hz, Ar_{meta}), 165.9 (ddd, $J = 7, 3, 2$ Hz, C-7), 166.8 (dd, $J = 4, 4$ Hz, Ar C=O), 167.3 (dq, $J = 4, 4$ Hz, CO₂CH₃); HRMS Calcd for C₁₇H₁₆N₂NaO₅S (M + Na) 383.0672, found 383.0674 (−0.5 ppm error); LC ($\lambda = 254$ nm) 19.176 min.

(2S, 5R, 6S)-6-(1,3-dioxoisindolin-2-yl)-3,3-dimethyl-7-oxo-4-thia-1-aza-bicyclo[3.2.0]heptane-2-carboxylic acid methyl ester (4)

¹H NMR (CDCl₃) δ 1.49 (s, 3H, α Me), 1.66 (s, 3H, β Me), 3.80 (s, 3H, CO₂CH₃), 4.64 (s, 1H, H-2), 5.41 (d, 1H, $J = 1.8$ Hz, H-6), 5.58 (d, 1H, $J = 1.8$ Hz, H-5), 7.79 (m, 2H, Ar_{meta}), 7.88 (m, 2H, Ar_{ortho}); ¹³C NMR δ 25.6 (qm, $J = 129$ Hz, α Me), 34.7 (qm, $J = 128$ Hz, β Me), 52.6 (q, $J = 148$ Hz, CO₂CH₃), 64.3 (br m, C-3), 64.5 (d, $J = 152$ Hz, C-6), 69.2 (ddd, $J = 178, 7, 4$ Hz, C-5), 69.4 (dm, 145 Hz, C-2), 124.1 (dm, $J = 166$ Hz, Ar_{ortho}), 131.7 (m, Ar_{ipso}), 134.9 (dd, $J = 165, 7$ Hz, Ar_{meta}), 166.6 (dd, $J = 4, 4$ Hz, Ar C=O), 167.4 (ddd, $J = 6, 4, 4$ Hz, C-7), 167.8 (dq, $J = 5, 4$ Hz, CO₂CH₃); HRMS Calcd for C₁₇H₁₆N₂NaO₅S (M + Na) 383.0672, found 383.0667 (−1.3 ppm error); LC ($\lambda = 254$ nm) 19.659 min.

(2S, 5R, 6R)-6-(1,3-dioxoisindolin-2-yl)-3,3-dimethyl-7-oxo-4-thia-1-aza-bicyclo[3.2.0]heptane-2-carboxylic acid (6)

¹H NMR (CDCl₃) δ 1.62 (s, 3H, α Me), 1.85 (s, 3H, β Me), 4.71 (s, 1H, H-2), 5.59 (d, 1H, $J = 3.9$ Hz, H-5), 5.70 (d, 1H, $J = 4.2$ Hz, H-6), 7.78 (m, 2H, Ar_{meta}), 7.90 (m, 2H, Ar_{ortho}); ¹³C NMR δ 28.2 (qm, $J = 129$ Hz, α Me), 30.5 (qm, $J = 129$ Hz, β Me), 58.4 (dd, $J = 151, 3$ Hz, C-6), 65.9 (br m, C-3), 66.8 (ddd, $J = 176, 3, 3$ Hz, C-5), 71.1 (dm, $J = 146$ Hz, C-2), 124.1 (dm, $J = 166$ Hz, Ar_{ortho}), 131.6 (m, Ar_{ipso}), 134.8 (dd, $J = 164, 7$ Hz, Ar_{meta}), 166.8 (dd, $J = 4, 4$ Hz, Ar C=O), 169.1 (ddd, $J = 9, 7, 5$ Hz, C-7), 172.6 (d, $J = 5$ Hz, CO₂H); HRMS Calcd C₁₆H₁₃N₂O₅S for (M − H) 345.0551, found 345.0544 (−2 ppm error); LC ($\lambda = 254$ nm) 16.934 min.

(2S, 5S, 6R)-6-(1,3-dioxoisindolin-2-yl)-3,3-dimethyl-7-oxo-4-thia-1-aza-bicyclo[3.2.0]heptane-2-carboxylic acid (7)

¹H NMR (CDCl₃) δ 1.57 (s, 3H, α Me), 1.73 (s, 3H, β Me), 4.03 (s, 1H, H-2), 5.39 (d, 1H, $J = 2.1$ Hz, H-5), 5.51 (d, 1H, $J = 1.8$ Hz, H-6), 7.78 (m, 2H, Ar_{meta}), 7.91 (m, 2H, Ar_{ortho}); ¹³C NMR δ 26.9 (qm, $J = 129$ Hz, α Me), 29.7 (qm, $J = 129$ Hz, β Me), 61.1 (d, $J = 153$ Hz, C-6), 65.2 (br m, C-3), 66.1 (ddd, $J = 177, 5, 3$ Hz, C-5), 72.2 (dm, $J = 152$ Hz, C-2), 124.2 (dm, $J = 167$ Hz, Ar_{ortho}), 131.6 (m, Ar_{ipso}), 135.0 (dm, $J = 165$ Hz, Ar_{meta}), 166.7 (dd, $J = 4, 4$ Hz, Ar C=O), 167.6 (d, $J = 5$ Hz, CO₂H), 168.8 (ddd, $J = 7, 4, 4$ Hz, C-7); HRMS Calcd for C₁₆H₁₄N₂NaO₅S (M + Na) 369.0516, found 369.0511 (−1.4 ppm error); LC ($\lambda = 254$ nm) 16.796 min.

(2S, 5R, 6S)-6-(1,3-dioxoisindolin-2-yl)-3,3-dimethyl-7-oxo-4-thia-1-aza-bicyclo[3.2.0]heptane-2-carboxylic acid (8)

¹H NMR (CDCl₃) δ 1.60 (s, 3H, α Me), 1.68 (s, 3H, β Me), 4.64 (s, 1H, H-2), 5.42 (d, 1H, $J = 1.8$ Hz, H-6), 5.56 (d, 1H, $J = 1.8$ Hz, H-5), 7.78 (m, 2H, Ar_{meta}), 7.90 (m, 2H, Ar_{ortho}); ¹³C NMR δ 25.8 (qm, $J = 129$ Hz, α Me), 34.3 (qm, $J = 129$ Hz, β Me), 64.2 (d, $J = 153$ Hz, C-6), 64.4 (br m, $J = 179$ Hz, C-3), 69.0 (dm, $J = 180$ Hz, C-5), 69.3 (dm, $J = 145$ Hz, C-2), 124.2 (dm, $J = 166$ Hz, Ar_{ortho}), 131.7 (m, Ar_{ipso}), 134.9 (dm, $J = 165, 7$ Hz, Ar_{meta}), 166.7 (dd, $J = 4, 4$ Hz, Ar C=O), 167.6 (ddd, $J = 7, 4, 4$ Hz, C-7), 172.0 (d, $J = 5$ Hz, CO₂H); HRMS Calcd for C₁₆H₁₃N₂O₅S (M − H) 345.0551, found 345.0536 (−4.3 ppm error); LC ($\lambda = 254$ nm) 16.841 min.

2-(5,5-dimethyl-2,5-dihydrothiazol-2-yl)-2-(1,3-dioxoisindolin-2-yl)acetic acid (9)

¹H NMR (CDCl₃) δ 1.54 (s, 3H, Me), 1.57 (s, 3H, Me), 4.83 (d, 1H, $J = 9.9$ Hz, H-2), 6.26 (dd, 1H, $J = 9.6, 2.3$ Hz, H-2'), 7.21 (d, 1H, $J = 2.1$ Hz, H-4'), 7.71 (m, 2H, Ar_{meta}), 7.83 (m, 2H, Ar_{ortho}); ¹³C NMR δ 29.0 (Me), 30.0 (Me), 57.9 (C-2), 64.4 (C-5'), 79.0 (C-2'), 123.9 (Ar_{ortho}), 131.8 (Ar_{ipso}), 134.4 (Ar_{meta}), 167.1 (ArC=O), 170.8 (COOH), 173.4 (C-4'); HRMS Calcd for C₁₅H₁₃N₂O₄S (M − H) 317.0602, found 317.0599 (−0.9 ppm error); and Calcd for C₁₅H₁₄N₂O₄SNa (M + Na) 341.0566, found 341.0560 (−1.8 ppm error); LC ($\lambda = 254$ nm) 15.240 min.

Supplementary material

Supplementary electronic material for this paper is available in Wiley InterScience at: <http://www.interscience.wiley.com/jpages/0749-1581/suppmat/>

Acknowledgements

This work was supported in part by the National Science Foundation (CJC, CHE-0203346) and the National Cancer Institute, National Institutes of Health (TRH, CA-76497).

REFERENCES

- Bagno A, Rastrelli F, Saielli G. *Chem. Eur. J.* 2006; **12**: 5514.
- Perez M, Peakman TM, Alex A, Higginson PD, Mitchell JC, Snowden MJ, Morao I. *J. Org. Chem.* 2006; **71**: 3103.
- Subramaniam G, Karimi S, Phillips D. *Magn. Reson. Chem.* 2006; **44**: 1118.
- Taubert S, Korschin H, Sundholm D. *Phys. Chem. Chem. Phys.* 2005; **7**: 2561.
- Baladina A, Mamedov V, Franck X, Figadere B, Latypov S. *Tetrahedron Lett.* 2004; **45**: 4003.
- Facelli JC. *Concepts Magn. Reson. Part A* 2004; **20A**: 42.
- Boggioni L, Bertini F, Zannoni G, Tritto I, Carbone P, Ragazzi M, Ferro DR. *Macromolecules* 2003; **36**: 882.
- Tahtinen P, Bagno A, Klika KD, Pihlaja K. *J. Am. Chem. Soc.* 2003; **125**: 4609.
- Price DR, Stanton JF. *Org. Lett.* 2002; **4**: 2809.
- Barone G, Gomez-Paloma L, Duca D, Silvestri A, Riccio R, Bifulco G. *Chem. Eur. J.* 2002; **8**: 3233.
- Ragazzi M, Carbone P, Ferro DR. *Int. J. Quantum Chem.* 2002; **88**: 663.
- Bagno A. *Chem. Eur. J.* 2001; **7**: 1652.
- Rich JE, Manalo MN, de Dios AC. *J. Phys. Chem. A* 2000; **104**: 5837.
- Kolehmainen E, Koivisto J, Nikiforov V, Perakyla M, Tuppurainen K, Laihia K, Kauppinen R, Miltsov SA, Karavan VS. *Magn. Reson. Chem.* 1999; **37**: 743.
- Ortiz PJ, Evleth EM, Montero LA. *J. Mol. Struct. (Theochem)* 1998; **432**: 121.
- Vogt FG, Spoor GP, Su Q, Andemichael YW, Wang H, Potter TC, Minick DJ. *J. Mol. Struct.* 2006; **797**: 5.
- Wipf P, Kerekes AD. *J. Nat. Prod.* 2003; **66**: 716.
- Harper JK, Barich DH, Hu JZ, Strobel GA, Grant DM. *J. Org. Chem.* 2003; **68**: 4609.
- Backes AC, Schatz J, Siehl H. *J. Chem. Soc., Perkin Trans. 2* 2002; **3**: 484.
- Barone G, Duca D, Silvestri A, Gomez-Paloma L, Riccio R, Bifulco G. *Chem. Eur. J.* 2002; **8**: 3240.
- Colombo D, Ferraboschi P, Ronchetti F, Toma L. *Magn. Reson. Chem.* 2002; **40**: 581.
- Monica CD, Randazzo A, Bifulco G, Cimino P, Aquino M, Izzo I, De Riccardis F, Gomez-Paloma L. *Tetrahedron Lett.* 2002; **43**: 5707.
- Ochsenfeld C, Brown SP, Schnell I, Gauss J, Spiess HW. *J. Am. Chem. Soc.* 2001; **123**: 2597.
- Brown SP, Schaller T, Seelbach UP, Koziol F, Ochsenfeld C, Klarner F, Spiess HW. *Angew. Chem. Int. Ed.* 2001; **40**: 717.
- Malkina OL, Hricovin M, Bizik F, Malkin VG. *J. Phys. Chem. A* 2001; **105**: 9188.
- Harper JK, Mulgrew AE, Li JY, Barich DH, Strobel GA, Grant DM. *J. Am. Chem. Soc.* 2001; **123**: 9837.
- Sebag AB, Friel CJ, Hansen RN, Forsyth DA. *J. Org. Chem.* 2000; **65**: 7902.
- Clark AJ, Ellard JM. *Tetrahedron Lett.* 1998; **39**: 6033.
- Stahl M, Schopfer U, Frenking G, Hoffman RW. *J. Org. Chem.* 1996; **61**: 8083.
- Cheeseman JR, Trucks GW, Keith TA, Frisch MJ. *J. Chem. Phys.* 1996; **104**: 5497.
- Cramer CJ. *Essentials of Computational Chemistry: Theories and Models*. John Wiley & Sons: Chichester, 2004.
- Wiitala KW, Hoye TR, Cramer CJ. *J. Chem. Theory Comput.* 2006; **2**: 1085.
- Migda W, Rys B. *Magn. Reson. Chem.* 2004; **42**: 459.
- Wang B, Hinton JF, Pulay P. *J. Comput. Chem.* 2002; **23**: 492.
- Wang B, Fleischer U, Hinton JF, Pulay P. *J. Comput. Chem.* 2001; **22**: 1887.
- Giesen DJ, Zumbulyadis N. *Phys. Chem. Chem. Phys.* 2002; **4**: 5498.
- Sebag AB, Forsyth DA, Plante MA. *J. Org. Chem.* 2001; **66**: 7967.
- Rablen PR, Pearlman SA, Finkbiner J. *J. Phys. Chem. A* 1999; **103**: 7357.
- Bifulco G, Dambruoso P, Gomez-Paloma L, Riccio R. *Chem. Rev.* 2007 (in press).
- Pretsch E, Bühlmann P, Affolter C. *Structure Determination of Organic Compounds: Tables of Spectral Data*. Springer: Berlin, 2004.
- Claridge T. *High-Resolution NMR Techniques in Organic Chemistry*. Elsevier: London, 2004.
- Becke AD. *Phys. Rev. A* 1988; **38**: 3098.
- Lee C, Yang W, Parr RG. *Phys. Rev. B* 1988; **37**: 785.
- Becke AD. *J. Chem. Phys.* 1993; **98**: 5648.
- Stephens PJ, Devlin FJ, Chabalowski CF, Frisch MJ. *J. Phys. Chem.* 1994; **98**: 11623.
- Perdew JP. In *Electronic Structure of Solids '91*. Ziesche P, Eschrig H (eds). Akademie Verlag: Berlin, 1991; 11.
- Perdew JP, Wang Y. *Phys. Rev. B* 1992; **45**: 13244.
- Kukolja S, Jones ND, Chaney MO, Elzey TK, Gleissner MR, Paschal JW, Dorman DE. *J. Org. Chem.* 1975; **40**: 2388.
- Fekner T, Baldwin JE, Adlington RM, Jones TW, Prout CK, Schofield CJ. *Tetrahedron* 2000; **56**: 6053.
- Kukolja S. *J. Am. Chem. Soc.* 1971; **93**: 6267.
- Fisher JW, Trinkle KL. *Tetrahedron Lett.* 1994; **35**: 2505.
- Chang CJ, Hem SL. *J. Pharm. Sci.* 1979; **68**: 64.
- Bodurov CC, Levy JN, Wiitala KW. *Tetrahedron Lett.* 1991; **33**: 4283.
- Schutz A, Ugi I. *J. Chem. Res. (S)* 1979; 157.
- Baldwin JE, Chan RY, Sutherland JD. *Tetrahedron Lett.* 1994; **35**: 5519.
- Diaz N, Suarez D, Sordo TL. *J. Comp. Chem.* 2003; **24**: 1864.
- Polak E, Ribiere G. *Rev. Franc. Informat. Rech. Oper.* 1969; **16**: 35.
- Chang G, Guides WC, Still WC. *J. Am. Chem. Soc.* 1989; **111**: 4379.
- Weiner SJ, Kollman PA, Case DA, Singh UC, Ghio C, Alagona G, Profeta S, Weiner P. *J. Am. Chem. Soc.* 1984; **106**: 765.
- Weiner SJ, Kollman PA, Nguyen DT, Case DA. *J. Comp. Chem.* 1986; **7**: 230.
- Still WC, Tempczyk A, Hawley RC, Hendrickson T. *J. Am. Chem. Soc.* 1990; **112**: 6127.
- Hehre WJ, Radom L, Schleyer PvR, Pople JA. *Ab Initio Molecular Orbital Theory*. Wiley: New York, 1986.
- Mennucci B, Tomasi J. *J. Chem. Phys.* 1997; **106**: 5151.
- Mennucci B, Cancès E, Tomasi J. *J. Phys. Chem. B* 1997; **101**: 10506.
- Tomasi J, Mennucci B, Cancès E. *J. Mol. Struct. (Theochem)* 1999; **464**: 211.
- Barone V, Cossi M, Tomasi J. *J. Chem. Phys.* 1997; **107**: 3210.
- London F. *J. Phys. Radium (Paris)* 1937; **8**: 397.
- Wolinski K, Hinton JF, Pulay P. *J. Am. Chem. Soc.* 1990; **112**: 8251.
- Gauss J. *J. Chem. Phys.* 1993; **99**: 3629.
- Cammi R. *J. Chem. Phys.* 1998; **109**: 3185.
- Cammi R, Mennucci B, Tomasi J. *J. Chem. Phys.* 1999; **110**: 7627.
- Bondi A. *J. Phys. Chem.* 1964; **68**: 441.
- Frisch MJ, Trucks GW, Schlegel HB, Scuseria GE, Robb MA, Cheeseman JR, Montgomery JA Jr, Vreven T, Kudin KN, Burant JC, Millam JM, Iyengar SS, Tomasi J, Barone V, Mennucci B, Cossi M, Scalmani G, Rega N, Petersson GA, Nakatsuji H, Hada M, Ehara M, Toyota K, Fukuda R, Hasegawa J, Ishida M, Nakajima T, Honda Y, Kitao O, Nakai H, Klene M, Li X, Knox JE, Hratchian HP, Cross JB, Bakken V, Adamo C, Jaramillo J, Gomperts R, Stratmann RE, Yazyev O, Austin AJ, Cammi R, Pomelli C, Ochterski JW, Ayala PY, Morokuma K, Voth GA, Salvador P, Dannenberg JJ, Zakrzewski VG, Dapprich S, Daniels AD, Strain MC, Farkas O,

Malick DK, Rabuck AD, Raghavachari K, Foresman JB, Ortiz JV, Cui Q, Baboul AG, Clifford S, Cioslowski J, Stefanov BB, Liu G, Liashenko A, Piskorz P, Komaromi I, Martin RL, Fox DJ, Keith T, Al-Laham MA, Peng CY, Nanayakkara A, Challacombe M, Gill PMW, Johnson B, Chen W, Wong MW,

Gonzalez C, Pople JA. *Gaussian 03, Revision B.05*, Gaussian: Wallingford, 2004.

74. Wiitala KW, Al-Rashid ZF, Dvornikovs V, Hoye TR, Cramer CJ. *J. Phys. Org. Chem.* 2007; **20**: 345.